Available online at www.sciencedirect.com
ScienceDirect
Journal of Hazardous Materials 153 (2008) 229–243
Journal of Hazardous Materials
www.elsevier.com/locate/jhazmat

Aspects of particulate dry deposition in the urban environment

Lage Jonsson [a,b,*], Edvard Karlsson [a], Pär Jönsson [b]

[a] FOI, Swedish Defence Research Agency, Division of CBRN Defence and Security, SE-901 82 Umeå, Sweden
[b] KTH, Royal Institute of Technology, SE-100 44 Stockholm, Sweden

Received 22 March 2007; received in revised form 17 August 2007; accepted 20 August 2007
Available online 31 August 2007

Abstract

Micro-scale deposition models, typically used for pipes, were adapted to outdoor situations and combined with computational fluid dynamics (CFD) calculations of flow conditions in order to study the fine structure of the deposition velocity on ground, walls, and roofs in an urban environment. Several deposition modeling techniques taken from the literature were used for the predictions. The urban geometry was represented by two different blocks of houses, which together with two wind directions gave four different cases to study. The calculations show large local variations of the deposition velocity resulting in a pattern similar to the variation of the friction velocity. This demonstrates the strong dependence of the deposition velocity on the friction velocity. Further alteration of the deposition velocity is caused by the variation of the micro-scale roughness and different surface temperatures. The results presented provide some guidance for where to look for hotspots of deposited material and also show that a representation of the deposition velocity in a city by only one or just a few values is a great simplification locally and could lead to serious mistakes.

Keywords: Dry deposition velocity; Deposition modeling techniques; Aerosol; Urbanized area; Hotspots

1. Introduction

Knowledge of the particulate dry deposition flux to outdoor surfaces in a city is needed for calculation of human exposure to aerosols. The particulate concentration followed by industrial release, vehicle emissions and from other human activities is influenced by the dry deposition. Walls of buildings and other surfaces may also be affected by the deposition and as a result be sooted and soiled. Release of hazardous aerosol or radioactive materials may cause a need for remediation of streets and walls of buildings, and the knowledge of the location of deposit would be valuable. Particles in cities have diameters in a wide range, ≈0.1–10 μm, often with a maximum around 2 μm [1]. Particle densities for soot-dominated particles are often around 1500 kg m^{-3} [2]. Biological hazardous aerosols have sizes between 1 and 10 μm [3] with densities around 1300 kg m^{-3} [4].

The method to calculate the dry deposition flux is normally based on the concept of the dry deposition velocity, v_d, with a corresponding deposition flux that equals v_d times the particle concentration. However, models and experiments for determining v_d of particulate fluxes onto typical surfaces in cities, e.g. walls of buildings and streets, are rare.

In the scientific literature, models for dry deposition of particles are presented especially for two areas, i.e. for pipe flows (often ventilation channels) and for air quality studies. The bases for deposition models for pipe flows normally is a diffusion equation which is integrated from the surface for smooth surfaces and from the micro-scale roughness height k_s (or some fraction of k_s) for rough surfaces [5]. k_s is defined as the mean height of the roughness elements. The parameter k_s often is some millimetres or less. The upper limit of integration is chosen to be outside the particle boundary layer. Deposition velocity will depend on k_s, friction velocity (in this context normally denoted by u_τ), particle size and density. Here, u_τ is defined as $\sqrt{(\tau/\rho)}$ where τ is the shear stress at the wall and ρ is the air density. Note, that u_τ is he same as u_* used in air quality studies.

The basis for deposition models for air quality models is also a diffusion equation, which is integrated from the surface through the canopy (normally vegetation) to a reference height above

* Corresponding author at: FOI, Swedish Defence Research Agency, Division of CBRN Defence and Security, SE-901 82 Umeå, Sweden.
Tel.: +46 90 10 68 36; fax: +46 90 10 68 02.
E-mail address: lage.jonsson@foi.se (L. Jonsson).

0304-3894/$ – see front matter © 2007 Elsevier B.V. All rights reserved.
doi:10.1016/j.jhazmat.2007.08.077

the canopy [6,7]. The result is formulated by using an aerodynamic resistance above the canopy and a surface resistance for the canopy. The aerodynamic resistance depends on reference height, canopy height (zero plane displacement), roughness height z_0, friction velocity u_* and atmospheric stability. The canopy resistance depend on the collection efficiency of the surface and is determined by various deposition processes; u_*, z_0, particle size and density and canopy type. Unlike the micro-scale roughness k_s, z_0 is not the mean height of the roughness elements, but instead about 10% of the roughness elements. Typical values of z_0 are 0.01 m (grass) to 1.0 m (forest, urban area). The canopy is treated as a unity and details within the canopy is not resolved. The parameter u_* is calculated from wind velocity above the canopy. Gravitational settling is also a part in both types of deposition models.

For *vertical surfaces* in ventilation channels there are three regimes of deposition determined by particle size, particle density, turbulence and surface roughness [5]: (i) for small particles (0–0.1 μm) there is a Brownian-turbulence diffusion regime with decreasing v_d for increasing particle size, (ii) for intermediate particle size there is a diffusion–impaction regime with increasing v_d for increasing particle size, and (iii) for the larger particles there is an inertia-moderated regime with slowly decreasing v_d for increasing particle size. Note, that for *horizontal surfaces* there will, in addition to the above mentioned regimes, be a gravity settling modification of v_d especially in the inertia-moderated regime.

Wells and Chamberlain [8] and Chamberlain et al. [9] made wind-tunnel experiments with smooth and rough surfaces, which show the three regimes for vertical surfaces described above. They found significantly larger v_d for the rough surfaces than for the smooth surfaces. Higher values of v_d were also measured to filter papers than to surfaces with widely spaced roughness elements. Liu and Agarwal [10] made experiments with similar results as Wells and Chamberlain [8] for smooth surfaces in pipes in the diffusion–impaction regime and the inertia-moderated regime. Sippola and Nazaroff [11] presented ventilation duct experiments for smooth and rough surfaces in the diffusion–impaction regime showing larger v_d for the rough surfaces (insulated ventilation ducts with micro-scale roughness height equal to 1.7 mm) than for the smooth surfaces (steel ducts) supporting the results of Chamberlain et al. [9].

Several papers present theoretical models for v_d in pipes (Friedlander and Johnstone [12], Davies [13], Wood [14], Fan and Ahmadi [15,16], Guha [17], Valentine and Smith [18], Zhao and Wu [19], Johansen [20]). In addition, Sippola and Nazaroff [5] have summarized the knowledge on particle deposition from turbulent flows in ventilation ducts. The main parameters influencing v_d is friction velocity, u_τ, particle size, particle density and micro-scale roughness height, k_s. Many of the existing models are applied to smooth (steel) surfaces, but the equations in some of the models can also be used for rough surfaces. For example, Gua presents result for both smooth and rough surfaces. The theory includes Brownian and turbulent diffusion, thermophoreses, turbophoreses, electrostatic forces, gravity and lift forces. For smooth surfaces existing models often agree relatively well between each other and with experimental data. However, for rough surfaces the agreement is worse. Therefore, Sippola and Nazaroff [11] derived a model in form of an interpolation formula based on their measured data.

Some authors have also reported experimental data of outdoor deposition. Offer and Goossens [21] and Erell and Tsoar [22] report wind-tunnel and field experiments on deposition of wind transported dust. They observed spatial variation especially in hilly terrain and where filter effects due to vegetation occurred. However, there was no determination of the spatial variation of flow parameters like u_τ and no correlation between flow parameters and deposition parameters were presented. Also, Simmons and Pocock [23] measured heavy metal particle flux to the surface in an urban area. They found that a large variability on a scale of 1 km could be explained by the release sources. On a smaller scale (<100 m) there was an additional variability of 90% (standard deviation divided by mean value), but the reason was not analyzed. The air flow conditions were not measured.

Although some experimental information on deposition is available, Monforti et al. [1] concludes that there exists "no experimental or deeper theoretical studies which focus on deposition on urban areas". They modeled particulate flux to cultural heritage sites in Florence Italy by using a multi-layer box model, but without resolving flow circulations in street canyons. The deposition velocity was calculated according to a procedure presented by Zhang et al. [7]. Calculated v_d for all suspended particles (weight maximum at 2 μm) ranged 0.05–0.8 cm s^{-1}, which seemed reasonable compared to observed range in urban areas (0.1–1 cm s^{-1}).

To account for the flow circulations, Benett [24] tries to formulate the effects of recirculation zones of a rough surface on the surface resistance by introducing a new term depending on the length scale for surface eddies. This term will increase the total resistance and can be used in deposition formulations using mean wind and roughness length z_0.

Gidhagen et al. [25] studied dispersion of ultra fine aerosols in a street canyon by coupling an aerosol model to a CFD model. The deposition model included Brownian diffusion, inertial impaction and gravitational settling, but could not be applied to smooth surfaces. They found that coagulation and deposition of ultra fine particles may reduce the concentration of particle concentration in the canyon by 30% at low wind speeds. However, no direct presentation of the particle deposition velocity was given.

Zhang et al. [7] has developed a dry deposition scheme for land areas, i.e. mainly for application over larger vegetated areas. The scheme includes turbulent transfer, Brownian diffusion, impaction, interception, gravitational settling and particle rebound. Their model also included the three regimes described above [5], together with the gravitational settling modification for horizontal surfaces. The model included 15 land use categories, one of which is urban, each with a predefined roughness length z_0 and radius of collectors. The model shows that the deposition velocity depends on surface type, friction velocity, particle density and particle size. The deposition velocity increases for rougher surfaces and higher u_τ. According to Fig. 1 in Zhang's paper a typical v_d is about 3 mm s^{-1} for 5 μm particles (2000 kg m^{-3}, 5 m s^{-1} at 20 m). However, the model is

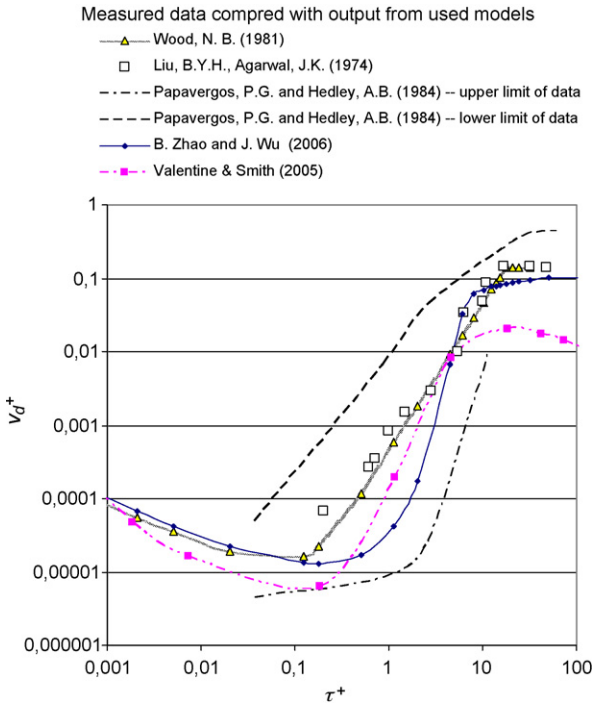

Fig. 1. The figure shows the agreement between the models used for smooth vertical surfaces and the measurements made by Liu and Agarwal, and Papavergos and Hedleys.

intended to be used without resolving the detailed flow around buildings and streets. The roughness parameter, $z_0 = 1.0$ m, is the large scale roughness parameter used together with a mean wind velocity above the buildings.

The deposition velocity is often strongly dependent on u_τ for most outdoor and tube models and experiments. Thus, a detailed modeling of v_d includes a detailed modeling of u_τ and its variation along streets, walls and roofs in the city. Since u_τ depends on geometry and flow conditions, a description of the streets, the buildings and the roughness of the surfaces is needed as well as the resolved fluid flow including turbulence conditions.

Besides influencing u_τ, the roughness of the surface influences the aerosol deposition by, for example, influencing the attachment to the surface. An increased micro-scale roughness height (k_s) increases v_d in those (few) tube models and experiments, which take into account the effect of roughness. Thus, the description of the surface in a city shall include the micro-scale roughness height of walls and roofs, with values between the extremes *complete smooth* (glass, metal $k_s = 0$) and *rough* (bricks, etc., k_s = several millimetres). Additionally, deposition models for outdoor surfaces often include impaction and interception effects, which depend on the radius of the collector, e.g. the radius of a tree needle. Even in cities there exist parts with vegetated surfaces with trees and grass and their collectors, in form of needles and leafs, should be defined. Probably, both u_τ and roughness will vary considerably along streets, parks, walls and roofs in a city but the question how v_d will vary remains.

In spite of just a few experiments for rough surfaces, there is a much better theoretical and experimental base for determining v_d in ventilation pipes compared to outdoor surfaces, i.e. walls, streets, roofs, etc. This is valid both for vertical and horizontal surfaces. Thus, adapting micro-scale deposition models, i.e. models intended for ventilation systems, to outdoor surfaces could render better tools for calculating v_d in the urban environment and provide tools for analyzing the probability of deposition-hotspots on different surfaces.

The purpose of this study is to illustrate the behavior of v_d in urban areas. To do this, CFD (computational fluid dynamics) simulations of flow conditions including u_τ were performed for different blocks of houses mimicking the urban environment. Knowing u_τ, calculation the magnitude, range and variation of v_d is possible by using deposition models reported in the literature.

2. Modeling

2.1. Modeling of dry deposition in the urbanized area

The dry deposition flux of particles from the atmosphere to a surface is governed by their concentration in the air, the turbulent and molecular transport in the boundary layer close to the phase boundary and by the chemical and physical nature of the depositing species (that determine how efficiently the surface can capture particles). To describe the exchange process v_d is usually used, as defined by the relation [26]

$$J = v_d C_\infty \tag{1}$$

where J is the flux of species to the surface, C_∞ is the concentration in the bulk flow. v_d provides a measure of conductivity between atmosphere and the surface capturing particles. Outdoor, in the urban environment, particles are deposited on walls, roofs and on the ground, where many of these surfaces are rough. To estimate the depositions of particles onto these surfaces, models of v_d are needed. Those pipe models which potentially could be used for rough surfaces and rather general conditions are of special interest in this context. Therefore, among the models available in the open literature, the following three deposition models have been selected: (i) Zhao and Wu [19] (supplemented with some ideas from Guha [17]), (ii) Valentine and Smith [18] and (iii) Wood [27] (with modification by Kvasnak and Ahmadi [28] to account for the effect of gravitational settling). For completeness and easy reference these models are shortly recapitulated in the following.

2.1.1. Deposition model by Zhao and Wu [19]

The model by Zhao and Wu [19] is an Eulerian model that is based on Ficks law and takes buoyancy and turbophoresis into account: It is based on the concept that there is a thin concentration boundary layer within the turbulent boundary layer leading to a modified form of Ficks law

$$J = -(\varepsilon_p + D_p)\frac{\partial C}{\partial y} - i v_s C + V_t C \tag{2}$$

where C is the particle concentration, y the coordinate normal to the wall, D_p the particle Brownian diffusion, ε_p the particle turbulent diffusivity, v_s the particle terminal velocity without influence of other external forces, V_t the turbophoretic velocity (calculated as given in reference [29]), and i is a discrete variable

that can take the values 1, 0, −1 depending on if the surface is directed upwards (floor), vertically or downwards (ceiling).

After introducing dimensionless variables (denoted by the superscript $^+$), Eq. (2) could be re-written

$$\frac{\mathrm{d}C^+}{\mathrm{d}y^+} + \left\{ iv_s^+ + \tau^+ \frac{\mathrm{d}\left[(\tau_L/(\tau_L+\tau_p))\overline{v_y'^2}^+\right]}{\mathrm{d}y^+} \right\} \left[Sc^{-1} + \left(\frac{\tau_L}{\tau_L+\tau_p}\right) v_t^+ \right]^{-1} C^+ = v_d^+ \left[Sc^{-1} + \left(\frac{\tau_L}{\tau_L+\tau_p}\right) v_t^+ \right]^{-1} \quad (3)$$

where τ_p and τ^+ are the particle relaxation time and the dimensionless particle relaxation time, respectively, τ_L the Lagrangian time scale, v_y' the wall-normal air velocity fluctuations and v_t^+ is the dimensionless eddy diffusivity in the air [30]. The details of the solution to the equation are given in reference [31]. Using the boundary condition $C^+(r^+)=0$ and $C^+(30)=1$ the normalized deposition velocity can be expressed as:

$$v_d^+ = \frac{F(30)}{\int_{r^+}^{30} F(y^+)[Sc^{-1} + (\tau_L/(\tau_L+\tau_p))v_t^+]^{-1}\mathrm{d}y^+} \quad (4)$$

where the extension of the buffer layer has been set to $y^+=30$. It could be noted that Guha [17] uses $y^+=200$, but numerical experiments up to $y^+=300$ revealed that this limit is by no means critical. F is a function of integration [19].

Eq. (4) can be solved numerically if functions are known for the air eddy diffusivity as well as for air velocity fluctuations normal to the wall. Following the procedure suggested by Zhao and Wu [19] to solve Eq. (4), empirical functions are used for the air eddy diffusivity [32] based on DNS simulations (direct numerical simulations in which all physical scales of the flow are resolved and no turbulence model is used) as well as for the RMS fluctuations (the quadratic mean fluctuations, a statistical measure of the magnitude of a varying quantity) in the wall-normal velocities [33] including corrections by Guha [17].

To apply this model for rough surfaces, a method originally proposed by Wood [14] and later recommended by Guha [17] is used, i.e. the lower limit of integration is modified to account for the roughness as follows

$$y_0^+ = 0.45k_s^+ + r^+ \quad (5)$$

where y_0^+ is the dimensionless lower limit of integration and k_s^+ is the dimensionless surface micro roughness.

Eq. (4) together with Eq. (5) is referred to as the Zhao and Wu model in the following.

2.1.2. Deposition model by Valentine and Smith [18]

The deposition model is based on the stop distance theory of Friedlander and Johnstone [12]. More specifically, a particle having an initial velocity V_0 in a quiescent fluid is assumed to travel a certain distance due to its inertia, i.e. the stop distance

$$S = V_0\tau_p \quad (6)$$

where V_0 is the particle velocity perpendicular to the wall at the edge of the viscous sublayer [34] and can be expressed as

$$V_0 = V_w + \frac{u_w'}{\sqrt{Sc_p}} \quad (7)$$

where u_w' is the wall-directed fluctuating velocity at the edge of the sublayer, V_w is the ballistic particle velocity. Further, Sc_p is the particle Schmidt number, i.e. the ratio of the fluid eddy diffusivity to the particle eddy diffusivity, which was analyzed by Tchen [35] assuming a homogenous turbulence field, which, according to Hinze [30] is a valid assumption for shear flows. Tchen found the following relationship:

$$Sc_p^{-1} = 1 + \left[\frac{1}{(\tau_f/\tau_p)^2 - 1}\right]\left[\frac{\mathrm{e}^{-t/\tau_p} - \mathrm{e}^{-t/\tau_f}}{1 - \mathrm{e}^{-t/\tau_f}}\right] \quad (8)$$

where t is the particle residence time and τ_f denotes the turbulence time scale which, assuming the buffer layer to extend to $\approx 24y^+$ and the characteristic buffer layer fluctuating velocity to be $u_w' = 0.4u_\tau$ [36], could be estimated as [18]

$$\tau_f = \frac{24\nu}{0.4u_\tau^2} \quad (9)$$

In the model by Valentine and Smith it is assumed[1] $t \approx \tau_f$, which, used in Eq. (8) above gives [34]:

$$Sc_p^{-1} = 1 + \frac{\mathrm{e}^{((-\tau_f/\tau_p)+1)} - 1}{1.72[(\tau_f/\tau_p)^2 - 1]} \quad (10)$$

Furthermore, the flux of particles through the buffer layer and the viscous sublayer is determined by

$$J = (D_p + \varepsilon_p)\frac{\mathrm{d}C}{\mathrm{d}y} \quad (11)$$

where D_p is the Brownian eddy diffusivity taken from Shimada et al. [37]. Making Eq. (11) non-dimensional, rearranging and integrating leads to

$$\frac{1}{V_D^+}\left[\int_{C^+(S^++r^+)}^{C^+=1} \mathrm{d}C^+\right] = \int_{(S^++r^+)}^{6} \frac{\mathrm{d}y^+}{(D_p/\nu + \varepsilon_p/\nu)} + \int_6^{30} \frac{\mathrm{d}y^+}{(D_p/\nu + \varepsilon_p/\nu)} = I_{vs} + I_{br} \quad (12)$$

Furthermore, it is assumed that at a distance $S^+ + r^+$ from the wall

$$C_{S^++r^+}^+ = \frac{V_D^+}{(V_0^+)_{S^++r^+}} \quad (13)$$

[1] For $t \ll \tau_p$ and $t \ll \tau_f Sc_p^{-1} = \tau_f/(\tau_f+\tau_p)$, for $t \gg \tau_p$ and $t \gg \tau_f Sc_p^{-1} = 1$.

Table 1
Recommended values of k_1, k_2 and k_3 for Eq. (15)

Investigator	k_1	k_2	k_3
Cleaver and Yates [38]	0.084		
Friedlander [39]	0.059		
Wood [27]	0.045	4.5×10^{-4}	0.13
Davies [40]	0.075		0.30
Papavergos and Hedley [41]	0.07	3.5×10^{-4}	0.18
Kneen and Strauss [42]		3.79×10^{-4}	
Liu and Agarwal [10]		6×10^{-4}	
Fan and Ahmadi [15]			0.14

which, substituted into Eq. (12) leads to

$$V_D^+ = \frac{1}{I_{vs} + I_{br} + 1/(V_0^+)_{S^+ + r^+}} \tag{14}$$

For known free stream and particle properties Eq. (14), in the following referred to as the *Valentine and Smith* model, can be evaluated for a specific surface micro roughness.

2.1.3. Empirical equations, deposition model by Woods [14,27]

The deposition across the entire range of particle sizes may be predicted by simple empirical equations and be applied to *vertical* surfaces across all deposition regimes when configured in the following manner [5]:

$$V_d^+ = k_1 Sc^{-2/3} + k_2 \tau^{+2} \quad \text{if} \quad k_1 Sc^{-2/3} + k_2 \tau^{+2} \le k_3 \tag{15}$$

$$V_d^+ = k_3 \quad \text{if} \quad k_1 Sc^{-2/3} + k_2 \tau^{+2} > k_3 \tag{16}$$

Table 1 summarizes different values for k_1, k_2 and k_3 found by different investigators.

To apply empirical equations of this type to *horizontal* surfaces, a simple modification to account for the effect of gravitational settling on the particle deposition velocity was added [28]. The result is

$$V_d^+ = k_1 Sc^{-2/3} + k_2 \tau^{+2} + g^+ \tau^+ \tag{17}$$

where g^+ is the dimensionless gravitational acceleration defined by

$$g^+ = \frac{g\nu}{u_\tau^3} \tag{18}$$

and g is positive for a floor and negative for a ceiling surface. In Eq. (17) the first term on the right hand side accounts for Brownian diffusion, the second term accounts for interactions between particle inertia and turbulent eddies and the final term accounts for gravitational settling. However, Eq. (17) does not account for surface roughness. In the following Eq. (17) is referred to as *Woods* model.

2.2. Comparison of models with focus on micro roughness

In Fig. 1, Wood, Zhao and Wu, and Valentine and Smith models for smooth vertical surfaces are compared to measurements by Liu and Agarwal [10], and Papavergos and Hedleys

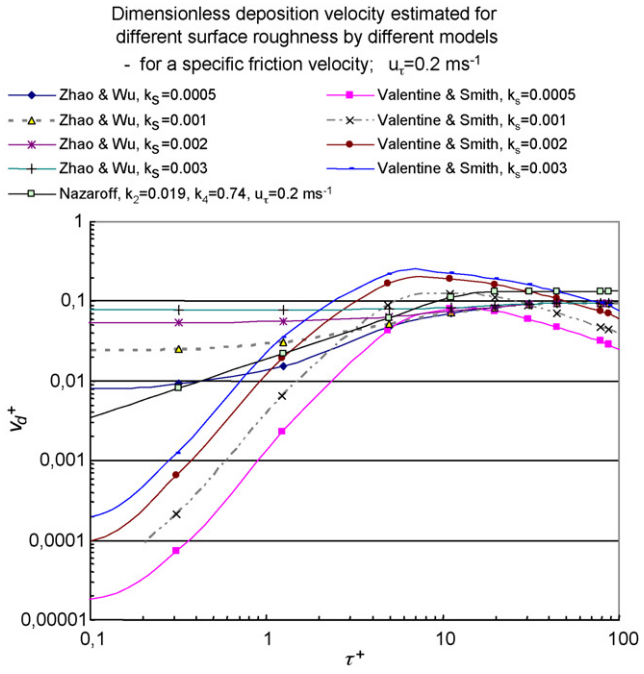

Fig. 2. The figure shows the dimensionless deposition velocity v_d^+ for rough vertical surfaces as a function of the dimensionless relaxation time τ^+ and different k_s as predicted by the models by Zhao and Wu, Valentine and Smith, and Nazaroff.

[41]. The three regimes described by Sippola and Nazaroff [5] are clearly observed. An acceptable agreement is also observed between predictions and measurements, especially for the model by Wood.

For rough vertical surfaces, in Fig. 2 the models by Zhao and Wu, and Valentine and Smith are compared with Nazaroffs empirical model [11], which is an adaptation to measurements with micro roughness $k_s \approx 0.0017$ m using equations similar to Wood (Eqs. (17) and (18)) but with exponents varying with u_τ. The figure shows that an increase in roughness $0.0005 \rightarrow 0.003$ increases the dimensionless deposition velocity approximately 10 times for small τ^+ up to $\tau^+ \approx 1$ and thereafter the increase lowers for increasing τ^+, at least up to $\tau^+ \approx 20$.

Comparing the different models with each other, the deviation in v_d^+ for a roughness = 0.003 between the model by Valentine and Smith and Nazaroff at $\tau^+ = 0.2$ and $\tau^+ = 20$ is seen to be $\approx$0.0068 (85% difference) and $\approx$0.06 (43%), respectively, while the corresponding values are 0.0079 (99%) and 0.06 (43%) for a roughness = 0.0005. The corresponding comparison with the model by Zhao and Wu results in 0.07 (88%) and 0.05 (36%) for $k_s = 0.003$. For $k_s = 0.0005$ the comparison renders a difference of 0.01 (12.5%) for $\tau^+ = 0.2$ and 0.05 (36%) for $\tau^+ = 20$. Furthermore, it is noted that for all $\tau^+ > 0.2$ predictions using the model by Zhao and Wu with $k_s = 0.0005$ renders similar results as those made by using the model by Nazaroff. Also, the predictions made by using the model by Valentine and Smith shows about the same agreement in the range $\tau^+ > 2$, though the shape of the curves are somewhat different.

In summary, there is a significant variation depending on the micro-scale roughness of the deposition surface, and some lack of agreement between the different models. Considering

any range of τ^+-values, it seems that the theoretical models for rough surfaces still suffers from large shortcomings, even though the results for smooth surfaces generally is seen to show agreement. If a restricted range of τ^+-values is considered ($2 < \tau^+ < 50$), the agreement between the different model predictions might be acceptable since the effect of roughness on different models' predictions does not vary too much in a limited interval and a smaller effect is found with larger particles.

2.3. Using the models for outdoor surfaces

All three models were originally developed for pipe flows. To use the models for outdoor conditions in an urban environment (walls, roofs, streets), they must be applied in conditions corresponding to those for their derivation. Thus, the roughness must be the micro-scale roughness k_s and not roughness length z_0, which is used for outdoor air quality deposition models in open terrain. Further, the flow and the friction velocity must be resolved to give representative values just above the particle boundary layers along walls, roofs and streets. However, if there is significant vegetation in the local area, these models should not be used. Instead the model by Zhang et al. [7] is recommended for such areas.

In present work, when coupling deposition models with CFD simulations in order to calculate v_d for urban environment, Woods model was used for *smooth horizontal and vertical surfaces*, because of acceptable agreement with measurements (Fig. 1) and simple equations (Eqs. (15)–(18)) giving acceptable computer times.

For *rough vertical* surfaces the model by Valentine and Smith was coupled to the CFD simulations because of acceptable agreement with measurements for larger particles (larger than $\tau^+ \approx 1$) and still acceptable computer times, something that could not be achieved using the model by Zhao and Wu. To illustrate deposition onto *rough horizontal* surfaces, Woods model was integrated into the CFD code, thereby requiring compensation for micro roughness at hand in any particular case. However, this compensation is moderate for particle sizes illustrated ($\tau^+ \approx 1$ giving diameter $\approx$5 μm) according to the previous discussion and Fig. 2, and, whatever micro roughness chosen to illustrate the conditions on different type of streets, sidewalks, etc., it would only be representative for a very specific case.

2.4. Modeling of fluid flow and turbulence by computational fluid dynamics

The theoretical model covers air flow in and around a block of houses. The mathematical model includes standard solutions of Navier–Stokes equations and turbulence as described in the following.

2.4.1. Mathematical formulation and boundary conditions

The following assumptions are made in the statement of the mathematical model:

(a) In each of the simulated cases the grid is Cartesian in a domain that has the shape of a parallelepiped.
(b) The upper limit of the domain is a flat frictionless surface at 300 m height.
(c) Pressure boundary conditions are used on three sides of the domain.
(d) The lower limit of the domain, i.e. the ground, is a fully rough surface with the surface roughness parameter z_0 for the logarithmic velocity profile set to 0.02 m to account for normal variability of the surfaces' structure. Furthermore, the standard logarithmic log-law is used for all surfaces of all buildings.
(e) At the inflow boundary a logarithmic wind-profile is applied with wind speed 4 m s^{-1} at 10 m height, i.e. mimicking a neutral stratification with wind speed 4 m s^{-1}.

2.4.2. Transport equations

In the mathematical model, the conservation of a general flow variable ϕ, for example momentum, enthalpy or species, within a finite control volume can be expressed as a balance between the various processes, which tend to increase or decrease the variable ϕ. This balance leads to a transport equation, which according to Patankar [43] has the following general form.

$$\frac{\partial}{\partial t}(\rho\phi) + \frac{\partial}{\partial x_i}(\rho\phi u_i) = \frac{\partial}{\partial x_i}\left(\Gamma_\phi \frac{\partial \phi}{\partial x_i}\right) + S_\phi \tag{19}$$

The first term expresses the rate of change of ϕ with respect to time, the second term expresses the convection (transport due to fluid flow), the third term expresses the diffusion (transport due to the variation of ϕ from point to point) where Γ_ϕ is the exchange coefficient of the entity ϕ in the phase. The fourth term expresses the source terms (associated with the creation or destruction of ϕ).

According to the mathematical formulation above the following governing transport equations must be solved:

- mass conservation;
- conservation of momentum in each co-ordinate direction;
- turbulence.

2.4.3. Turbulent transport equations

The equations for the turbulent kinetic energy and the dissipation rate of the turbulent kinetic energy from the well-known k–ε model [44] have been used with the source terms modified [45,46].

2.4.4. Property variations

The density for air is calculated using the assumption of an ideal gas. Thus, the gas is compressible. The density and the dynamic molecular viscosity of air at 0 °C were used in the calculations.

2.4.5. Geometry of blocks

Four geometric cases are simulated, referenced as "square houses 90 degrees", "square houses 45 degrees", "long houses 90 degrees" and "long houses 45 degrees". Both geometries

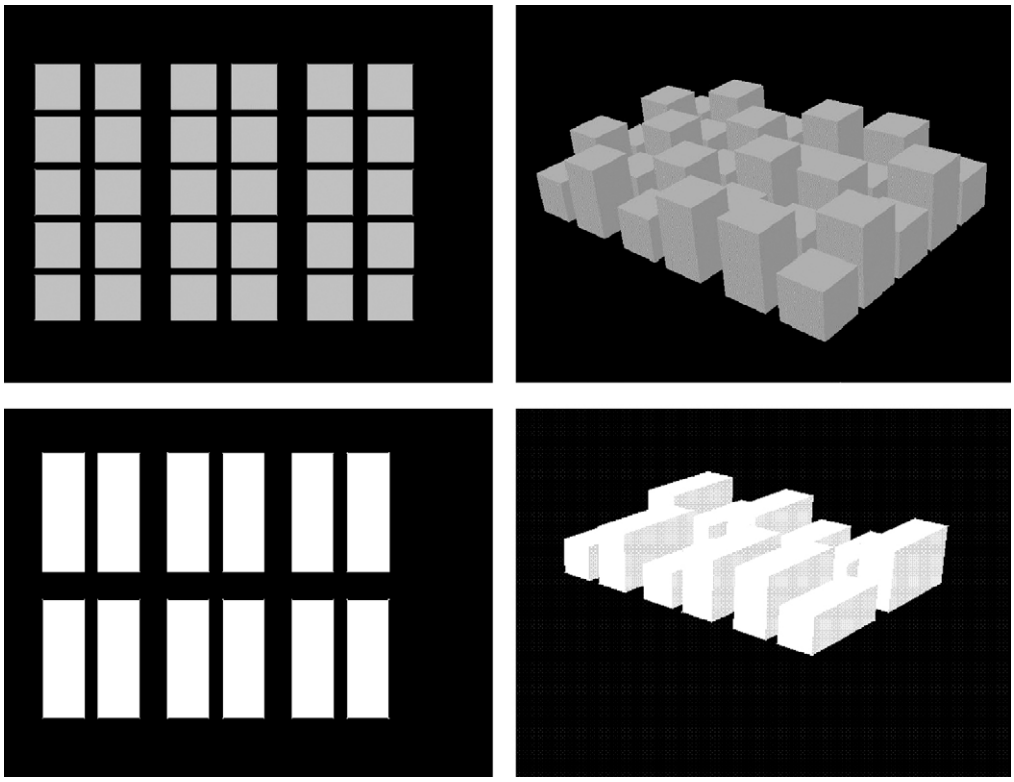

Fig. 3. The figure illustrates the four simulated geometric cases, referenced as "square houses 90 degrees" (upper left), "square houses 45 degrees" (upper right), "long houses 90 degrees" (lower left) and "long houses 45 degrees" (lower right). Both geometries called "square houses" are the same topographic configuration, the only difference being that in one case (upper left) the incoming wind is perpendicular towards the block, and in the other case the wind incident angle is 45° (upper right). The same applies for "long houses".

called "square houses" are the same geometric configuration, the only difference being that in one case the approaching wind, which is aligned along the x-axis, is perpendicular towards the block, where in the other case the approaching wind angle of incidence is 45°. The same applies for "long houses".

The block of "square houses" are made up of parallelepipeds 30 m × 30 m in the ground plane in six rows where each second house is 30 or 50 m high, except in between row 4 and 5 where houses of equal height faces each other in the wind direction. Each row consists of five houses abreast; see uppermost pictures in Fig. 3. Each second distance between "square houses" is 10 or 20 m in the flow direction and 10 m in the cross-flow direction, respectively.

The block of "long houses" are made up of parallelepipeds 30 m × 90 m in the ground plane in six rows where each second is 30 or 50 m high, except in between row 4 and 5 where houses of equal height faces each other in the wind direction. Each row consists of two houses abreast; see lowermost pictures in Fig. 3. Each second distance between "long houses" is 10 or 20 m in the flow direction and 20 m in the cross-flow direction, respectively.

2.5. Estimation of friction velocity

In this investigation, two approaches have been used to estimate the friction velocity. In both approaches the fluid flow conditions are needed, here calculated for the geometries in Fig. 3 by CFD.

To illustrate typical local values on walls, roofs and on the ground, denoted u_τ, the friction velocity is calculated as [18]

$$u_\tau = \sqrt{\mathrm{KE}\sqrt{0.09}} \tag{20}$$

where KE is the turbulent kinetic energy next to the surface/wall.

However, in air quality studies at neutral stratification a mean friction velocity is normally denoted u_* and calculated by the following equation[2] (similarity theory)

$$u_* = \frac{K u_\mathrm{r}}{\ln((z_\mathrm{r} - d)/z_0)} \tag{21}$$

where K is von Karmans constant, u_r the reference velocity at the reference height z_r (above the block of buildings), z_0 the roughness height (comp. paragraph 1) and d is the zero-plane displacement.

3. Results

Four geometric cases are simulated: (i) "square houses 90 degrees", (ii) "square houses 45 degrees", (iii) "long houses 90 degrees" and (iv) "long houses 45 degrees".

[2] Note, however, that that the block of buildings should be large enough to give horizontal homogeneity.

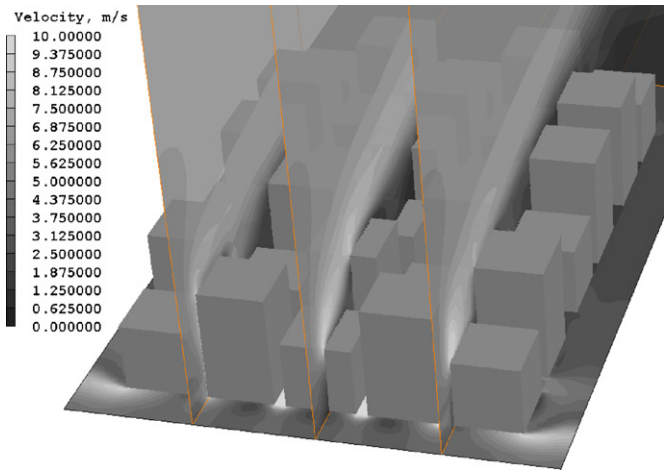

Fig. 4. The figure shows velocity contours in three vertical planes in the flow direction (two planes along streets and the middle plane right across the middle house) and at the ground plane for "square houses" faced 90° towards the wind direction. Note that the flow exiting to the right from the first cross road is perpendicular to the incoming wind. Also, the wind speed increases when the air enters streets aligned in the wind direction.

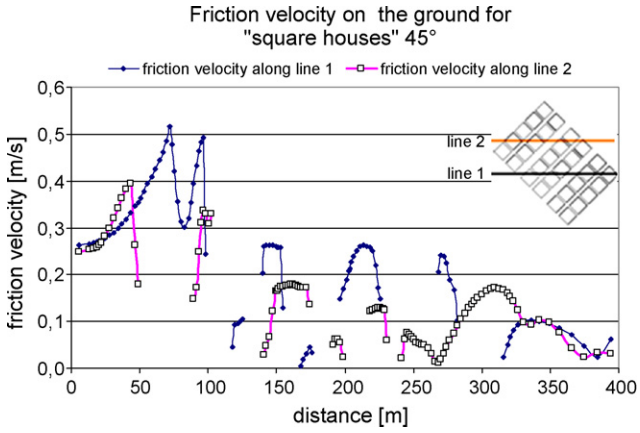

Fig. 5. Friction velocity *on the ground* presented in a cross-section along the indicated two lines for "square houses" 45°.

3.1. Flow conditions

The three-dimensional flow conditions in the block of houses are rather complex and difficult to illustrate. A detailed study of the flow field reveals recirculation zones on the roof tops, at the front building fronts, building-sides and in the downstream cavity regions, much like the illustration by Hosker [47], and also on- and off-axis channeling effects [48]. The length and height and size of the recirculation regions and their orientation are dependent on building heights, widths, downwind lengths and wind angles, resembling the suggestions derived from atmospheric and wind-tunnel experiments by Röckle [49]. Some features of the flow are shown in Fig. 4, where velocity contours for "square houses" faced 90° towards approaching wind is presented along three vertical planes and also on the ground plane.

3.2. Friction velocity

"Typical" and "high" calculated friction velocities on walls, roofs and ground are presented in Table 2. The friction velocity varies up to a factor of seven between "typical" and "high" velocities. Curves of u_τ on ground and roofs for "square houses

Table 2
"Typical" and "high" values of friction velocity, u_τ, for a block of "buildings" made up of "square houses" (30 and 50 m high parallelepipeds with base 30 m × 30 m, see upper part of Fig. 3) and "long houses" (30 and 50 m high parallelepipeds with base 30 m × 90 m, see lower part of Fig. 3)

Typical values
Estimated friction velocity from *turbulent kinetic energy* for different blocks of buildings

Place	Blocks of "square houses"				Blocks of "long houses"			
	Faced 90° towards approaching wind		Faced 45° towards approaching wind		Faced 90° towards approaching wind		Faced 45° towards approaching wind	
	KE[a]	Friction velocity u_τ[b]	KE[a]	Friction velocity u_τ[b]	KE[a]	Friction velocity u_τ[b]	KE[a]	Friction velocity u_τ[b]
Front wall first block	High 7 Typical 0.13	1.44 0.20	High 2 Typical 0.2	0.77 0.25	High 0.3 Typical 0.12	0.3 0.19	High[c] >0.3 Typical 0.08	≥0.3 0.16
Front wall second block	High 0.7 Typical 0.06	0.45 0.14	High 2 Typical 0.22	0.77 0.26	High 1 Typical 0.22	0.54 0.26	High 0.3 Typical 0.08	0.3 0.16
Front wall third block	High 1 Typical 0.02	0.54 0.08	High 1.5 Typical 0.19	0.67 0.24	High 0.3 Typical 0.08	0.3 0.16	High 0.3 Typical 0.07	0.3 0.15
On the roofs	High 1.6 Typical 0.13	0.69 0.20	High 4 Typical 0.08	1.09 0.16	High 5 Typical 0.13	1.22 0.2	High 2(corner) Typical 0.14	0.77 0.21
On the ground	High 4 Typical 0.45	1.09 0.37	High 1(corner) Typical 0.4	0.54 0.34	High 0.3 Typical 0.3	0.3 0.31	High >0.3 Typical 0.27	≥0.3 0.29

Friction velocity values are estimated using the turbulent kinetic energy close to the wall/ground/roof. The "typical" values of u_τ are calculated from area mean values of turbulent kinetic energy.

[a] Derived value of turbulent kinetic energy, KE, from CFD.

[b] Estimated friction velocity u_τ using the derived value of KE (Eq. (20)).

[c] Upper edge 0.17, vertical edge 0.27, ground level >0.3.

Table 3
Heuristic comparison of estimated friction velocity values calculated by similarity theory (u_*, Eq. (21)) and "typical" local values (Table 2 derived by fluid flow (u_τ, Eq. (20))

Heuristic comparison of estimated friction velocity values calculated by similarity theory (u_*) and "typical" local values derived by fluid flow (u_τ)				
Case/geometry	Horizontally homogenous values derived by *similarity theory*		Local values derived by *fluid flow* (CFD)	
	z_0[a] (m)	u_* (m s^{-1})	Wind velocity at ref height (m s^{-1})	u_τ (m s^{-1})
Blocks of "square houses"				
Faced 90° towards approaching wind	2.1	0.65	3.7	0.08–0.37
Faced 45° towards approaching wind	1.6	0.66	4.2	0.16–0.34
Blocks of "long houses"				
Faced 90° towards approaching wind	1.5	0.77	5.06	0.16–0.31
Faced 45° towards approaching wind	1.5	0.70	4.6	0.15–0.29

The zero plane displacement d in Eq. (21) is taken as $0.7^* h_m = 28$ m, where h_m is the average height of the buildings. Reference height is 50 m, which equals the top of the highest buildings.

[a] z_0 is calculated as the volume of all buildings divided by the area of the domain.

45 degrees" in a cross-section along two lines are presented in Figs. 5 and 6. The variation with distance is fast (steep curves in Figs. 5 and 6) and the steepest gradients are often found near the boarders of the buildings. There is also a general trend of a decrease in friction velocity with distance in the wind direction as well as lower u_τ at lower roofs. To get some insight into how the resolved values of friction velocity are related to overall characteristics, Table 3 presents the calculated values of the local friction velocity, u_τ, for walls, roofs and on the ground, heuristically compared to the friction velocity in the form normally used in air quality studies at neutral stratification, u_*.

3.3. Variation of deposition velocity with particle size, particle density, surface micro roughness and temperature

In Figs. 7–9 deposition velocities in the building blocks are presented using the "typical" friction velocity values (from kinetic energy data) given in Table 2 for the blocks of houses. The deposition model by Zhao and Wu [19] was used with some comparison with the model by Wood.

In Fig. 7 typical deposition velocities on vertical smooth walls (comparable to steel or glass) for three particle densities are plotted as a function of particle size. The figure shows that the influence of particle density is minor for small particles ($d < 5$ μm) as well as for large particles ($d > 25$ μm). However, in the interval 5 μm $< d <$ 25 μm the influence of density is significant. For example, the deposition velocity of 3000 kg m^{-3} particles could be 60 times higher than the deposition velocity for 1300 kg m^{-3} particles. The model by Wood (only 1300 kg m^{-3} particles are presented) differs from Zhao and Wu for particle sizes 5–25 μm.

In Figs. 8 and 9 typical deposition velocities on the ground and on roofs for different micro roughness are plotted as a function of particle size for the specific particle density 1300 kg m^{-3}. The effect of micro roughness is largest for the smallest particles as shown in Fig. 2. The lower v_d on roofs depends on lower typical u_τ (Table 2). The model by Wood (smooth surface) agrees with Zhao and Wu.

According to the model by Valentine and Smith [18], the temperature dependence of v_d is not significantly influenced by surface micro roughness. For conditions representative for the front walls in the four cases studied, Table 4 presents the calculated change of the particle deposition velocity per degree Centigrade.

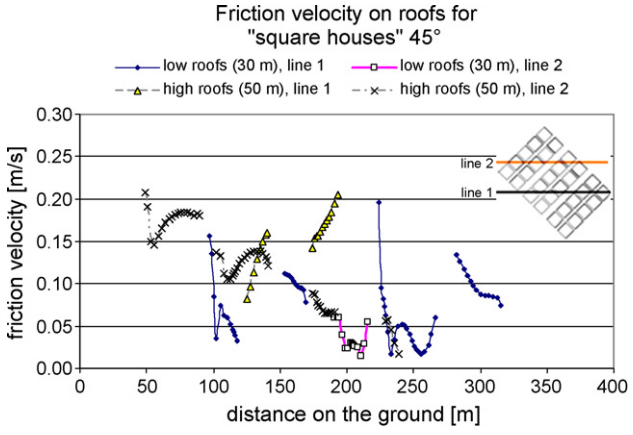

Fig. 6. Friction velocity *on high and low roofs* presented in a cross-section along the indicated two lines for "square houses" 45°.

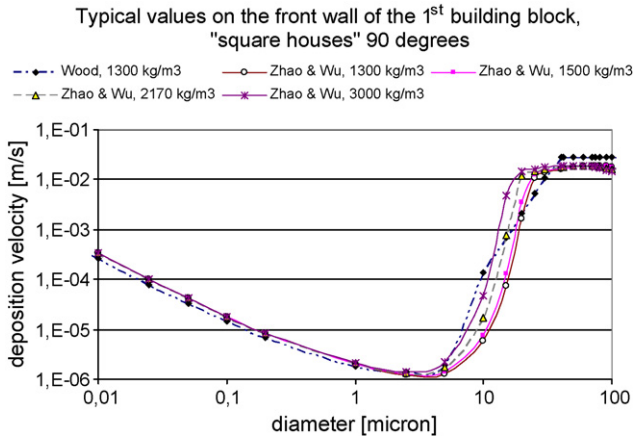

Fig. 7. Typical deposition velocity presented as a function of particle diameter and particle density for a smooth vertical wall. Friction velocity used for v_d from Table 2.

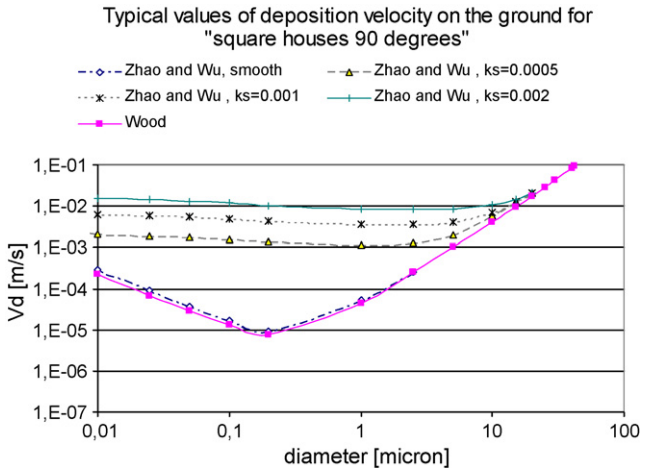

Fig. 8. Typical deposition velocity on the ground presented as a function of the diameter of particles (1300 kg m^{-3}) and surface micro roughness. Data from Table 2 was used for calculation of v_d.

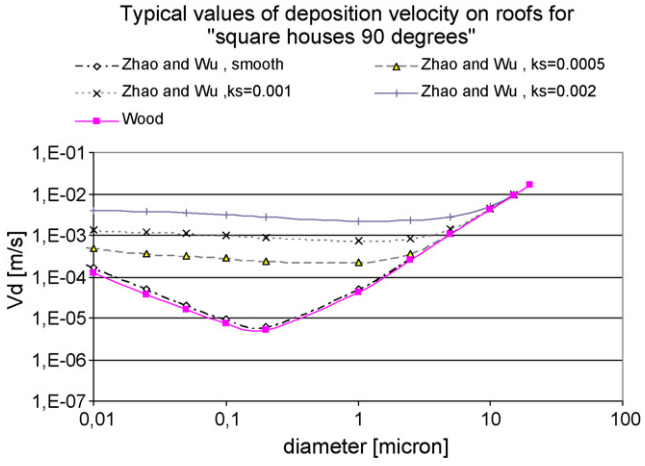

Fig. 9. Typical deposition velocity on roofs presented as a function of the diameter of particles (1300 kg m^{-3}) and surface micro roughness. Data from Table 2 was used for calculation of v_d.

3.4. Deposition velocity in the blocks of houses

Calculation of deposition velocity on ground, roofs and walls were made in order to illustrate the effect of flow conditions in a complex geometry, like a block of houses in a city, on v_d, e.g. magnitude, range and variation with distance. The aim was not to present results for specific cases but rather to illustrate probable ranges, dependencies and structures of v_d, since any topography would not be generic. Furthermore, a detailed description/knowledge of the surface micro-scale roughness did not exist and the available deposition models exhibit limitations as described above. Fully integrated with CFD, v_d was calculated for:

Rough vertical walls	by the model "Valentine and Smith" using $k_s = 0.0015$ m
Smooth horizontal roofs	by the model "Wood"
Smooth horizontal ground	by the model "Wood"

Table 4
Increase of v_d/°C for warmer air and cooler wall calculated for conditions representative for the front wall of "square houses 90 degrees", "square houses 45 degrees", "long houses 90 degrees" and "long houses 45 degrees"

Geometry	0.1 μm	1 μm	5 μm
"square houses 90 degrees"	7.34×10^{-8}	$7{,}34 \times 10^{-8}$	$2{,}99 \times 10^{-7}$
"square houses 45 degrees"	1.14×10^{-7}	1.27×10^{-8}	4.57×10^{-7}
"long houses 90 degrees"	6.89×10^{-8}	1.27×10^{-7}	2.76×10^{-7}
"long houses 45 degrees"	4.86×10^{-8}	8.97×10^{-8}	1.96×10^{-7}

Data from Table 2 was used and a thermal boundary layer with thickness $300y^+$ was assumed, density 1300 kg m^{-3}.

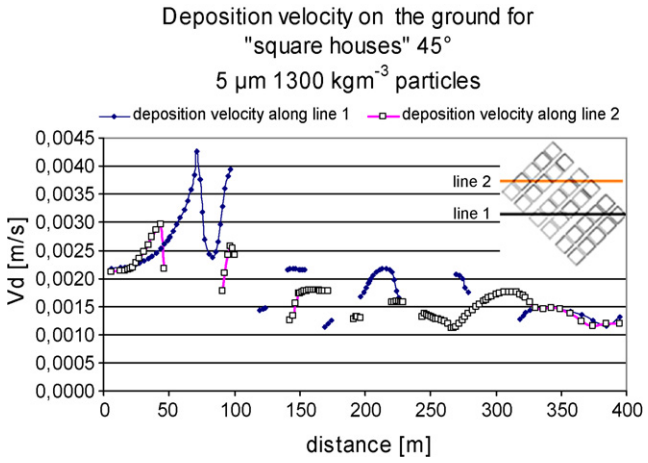

Fig. 10. Deposition velocity on the ground presented in cross-sections along the indicated two lines for "square houses" 45°. The curves are drawn for particles having a diameter 5 μm and a density 1300 kg m^{-3}.

The particle size used for illustrations is 5 μm with a particle density of 1300 kg m^{-3}. A neutral fully rough ($z_0 = 0.02$ m) wind profile of 4 m s^{-1} with the wind direction perpendicular, or alternatively 45°, to the front walls, is assumed for all cases. The chosen type of particles represents a biological hazardous aerosol, e.g. bacteria.

Figs. 10 and 11 shows v_d on ground and roofs presented in cross-sections along the same two lines as for u_τ (Figs. 5 and 6).

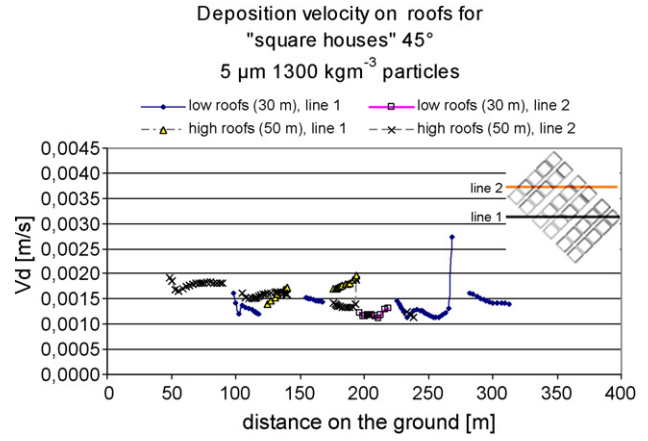

Fig. 11. Deposition velocity on high and low roofs presented in cross-sections along the indicated two lines for "square houses" 45°. The curves are drawn for particles having a diameter 5 μm and a density 1300 kg m^{-3}.

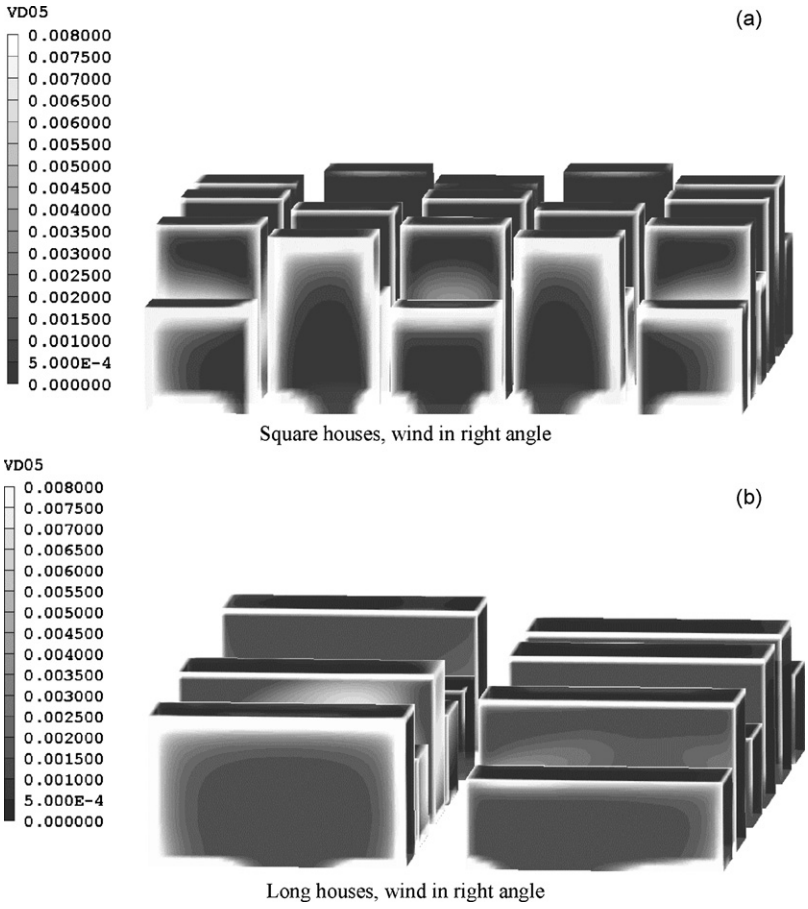

Fig. 12. Contours of deposition velocity v_d (m s^{-1}) on front walls according to the model by Valentine and Smith (micro roughness $k_s = 0.0015$, density $\rho = 1300\,\mathrm{kg\,m^{-3}}$) for $d = 5\,\mu\mathrm{m}$ particles, neutral stratification 4 m s^{-1}, wind in right angle towards the houses and fully rough ground (0.02). (a) Shows the situation for a group of "square" houses 30 m × 30 m × 30/50 m where the incoming wind is directed perpendicular towards the front walls and (b) shows the same for a group of "long" houses 30 m × 90 m × 30/50 m. Note that the highest value of the scale represents $v_d \geq 0.008\,\mathrm{m\,s^{-1}}$, i.e. the scale is chosen to be able to show the variation and does not represent max.–min. values.

Calculated v_d contours on the first front wall towards the wind are presented in Fig. 12 and v_d contours on the ground are presented in Fig. 13. The deposition velocity varies considerably and fast similar to u_τ, showing the strong dependence between v_d and u_τ. The variation of v_d in Figs. 10 and 11 is 1–4 mm s^{-1}. The variation of v_d in Fig. 12 is 0.5–8 mm s^{-1} over much of the surfaces, but close to the edges higher values are found and also at the lower boundaries of the buildings where v_d increases to several cm s^{-1} close to the ground near the corners (these values can not be seen in the plot because it occurs only over a smaller area and are outside the chosen scale). The pattern observed in both Fig. 12a and b, i.e. that v_d increases on front walls towards the edges and also towards the ground (in particular closer to the front corners), is more general and does indeed seem to be valid for any approaching wind angle. However, the variation of v_d on the interior of the wall surface is different. This variation becomes smaller with a smaller angle of the incoming wind.

The range in Fig. 13 is 0.2–2 mm s^{-1} where the high values are concentrated in certain areas depending on wind angle. Yet much higher values (about 6 cm s^{-1}, not seen in the plot because of the chosen scale) exist in hotspots found on both sides of the middle house in the front row and at both front corners of the whole building block in Fig. 13a and also near the front corners of the high house in the front row in Fig. 13c. Furthermore, the average deposition velocity on the ground within the block of houses is, due to the contribution from locally high values of v_d, 10–30% higher for groups of houses perpendicular to the approaching wind (Fig. 13a (0.0022 m s^{-1}) and c (0.0026 m s^{-1})) than for groups faced 45° towards the approaching wind (Fig. 13b (0.0020 m s^{-1}) and d (0.0018 m s^{-1})). Thus, the highest average v_d on the ground is found for "long houses" faced 90° towards the wind (Fig. 13c).

4. Discussion

4.1. Flow conditions

The calculated flow patterns for the four specific configurations (Fig. 3) could be expected to be sufficiently correct for the purpose of this investigation considering that, among others, Chang and Meroney [50], have showed that predictions using the k–ε turbulence model were in good agreement with experimental data regarding ensemble or time average flow features

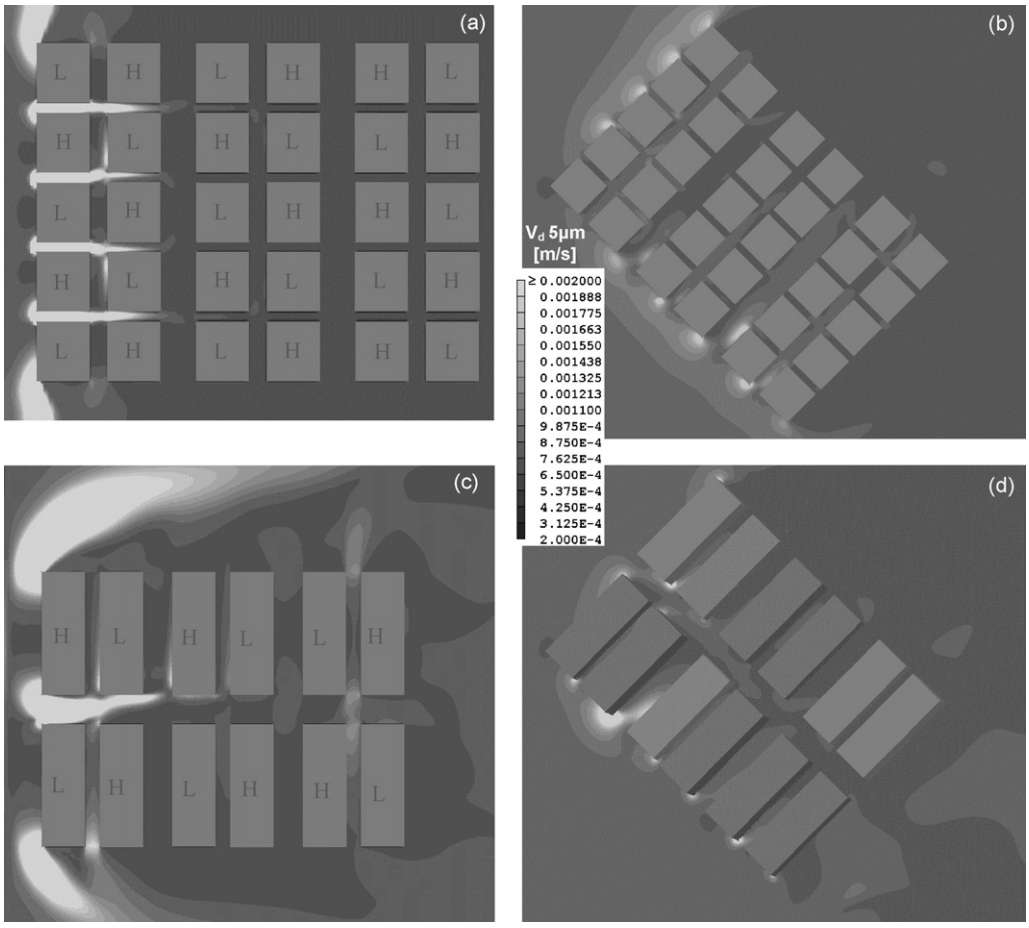

Fig. 13. The figure shows the deposition velocity pattern on the ground for $d = 5$ μm particles (1300 kg m^{-3}) using the model by Wood (smooth, e.g. negligible micro roughness) and an approaching wind 4 m s^{-1} (wind direction from left to right). The letters "H" and "L" denotes "high" houses (50 m) and "low" houses (30 m). (a) Shows the situation for a group of "square" houses 30 m × 30 m × 30/50 m where the approaching wind is directed perpendicular towards the front walls and (b) shows the same but with the approaching wind directed 45° towards the front walls. (c) Shows the situation for a group of "long" houses 30 m × 90 m × 30/50 m where the approaching wind is directed perpendicular towards the front walls and (d) shows the same as (c) but with the approaching wind directed 45° towards the front walls. Note that the highest value of the scale represents $v_d \geq 0.002$ m s^{-1}, i.e. the scale is chosen to be able to show the variation and does not represent max.–min. values. To get a reference to absolute values, compare (b) and Fig. 10.

that develops around 3-D buildings in a boundary layer flow. Furthermore, the present results reflect most of the significant features that can be found in several related wind-tunnel experiments [49–52] and towing tank experiments [53]. Moreover, the assumption of a neutral approach flow should not seriously restrict the validity of the results as Zhang, Arya and Snyder [54] showed that the stratification will rarely be a significant factor influencing the flow structure in the near-vicinity of a building.

However, the four specific configurations (Fig. 3) were chosen only to be able to illustrate specific features of the dry deposition and thus do not have any generic validity. Other flow conditions will be prevailing for another topography, other weather situations, etc. Furthermore, vehicle movements may significantly influence turbulence and air streams as shown by Gidhagen et al. [25], thereby often increasing u_τ and v_d. This effect is not currently included, but any future investigation could add this effect to study its influence on v_d.

4.2. Friction velocity

The locally calculated friction velocity u_τ for walls, roofs and the ground is only ∼25–55% of the mean friction velocity u_* in the form normally used in air quality studies (Table 3). It is reasonable to expect a higher value for u_* since both u_* and u_τ represents the flux of momentum perpendicular to the surface, but the surfaces for u_* are roofs and ground and the surfaces for u_τ are *walls*, roofs and ground. Thus, the total surface for u_* is much smaller and therefore u_* has a higher value.

4.3. Deposition velocity

The flow conditions have a strong influence on the deposition through the influence of wind velocity on u_τ and in turn on v_d. The variation of v_d in Figs. 10–13 therefore reflects the variation of wind and u_τ in the blocks of houses. This picture is expected to show a main behavior of v_d in spite of using Wood's model also for such horizontal surfaces which in reality could be expected

to be rough, thereby somewhat underestimating v_d for these surfaces.

Furthermore, according to Fig. 2, Figs. 8 and 9, which can be used to judge the influence of micro roughness at hand in any particular case, a larger variation of v_d is expected in any surrounding area since a typical surface can be made up of both more rough pieces (brick and asphalt) and smooth pieces (glass, steel).

The results indicates that choosing just one or only a few v_d-values in a city is a great simplification on the local scale and could lead to serious errors when calculating deposition at that scale.

In addition to the results presented, many more calculations of v_d were made for the two building blocks and the two wind angles, among them calculations for several particle sizes, for example 5, 10 and 20 μm particles with density 1300 kg m^{-3}. The range of v_d varies a lot between different particle sizes. For instance, v_d-maximum on ground was ≈6 cm s^{-1} for 5 μm and ≈0.5 m s^{-1} for 10 μm. v_d-maximum on roofs were ≈1 cm s^{-1} for 5 μm and ≈14 cm s^{-1} for 10 μm. These maxima were concentrated to limited areas emphasizing the view of a large and quick variation of v_d especially near edges of houses. Details of these simulations was not included as part of an effort to reduce the length of the paper.

The effect in the urban area of the surface orientation (vertical wall–horizontal surface) on the deposition velocity on a smooth surface can be studied by comparing Fig. 7 with Figs. 8 and 9. For smooth vertical walls (Fig. 7) v_d is lower than for smooth horizontal surfaces (Figs. 8 and 9). Furthermore, the minimum for v_d is reached at a higher particle diameter for the vertical surface in comparison with the two horizontal surfaces. For particle diameters 1–10 μm the difference in v_d between vertical and horizontal smooth surfaces is larger than one order of magnitude. Mainly the effect is caused by gravitational influence. However, for particle diameters less than 0.1 μm this difference is small.

Calculated values of v_d in Figs. 10–13 (modified for the differences in height above the surface) in general agrees with often reported values in cities (0.1–1 cm s^{-1}) [1] and with the results from Zhang et al.'s model [7] for particles around 5 μm, except for the isolated hotspots. However, no experimental investigation seems to have studied these maxima. The measurements of Simmons and Pocock [23] show large variations of particle flux to the surface on a scale less than 100 m supporting the results in Figs. 10–13. Conversely, any investigation does not seem to exist which has studied the deposition on an even smaller scale, which could verify the fine structure in Figs. 10–13.

Due to the buildings good electric earth connection, electrostatic forces, which were excluded in the calculations, in most cases are believed to be of minor importance, except for glass surfaces in dry weather. Though, thermophoreses may be more important. A rough calculation using the model by Valentine and Smith [18] on vertical surfaces (Table 4) shows that v_d could be strongly reduced, perhaps to zero, for a surface which is smooth and has a 10 °C higher temperature than air. On the other hand, v_d is significantly increased for a surface which has a temperature that is 10 °C lower than air.

For weather conditions other than those used in this study (wind 4 m s^{-1}, neutral stratification) the predicted deposition velocity will, of course, be different, but the main results showing large variations of v_d is believed to be similar when varying the conditions. Note that the influence of vegetation in cities and the effect of wet surfaces were not taken into account in the present study.

When calculating the dry deposition velocity, the underlying intention normally is to calculate the flux of particles to the surface according to $J = v_d C_\infty$ (Eq. (1)), where C_∞ is the bulk flow concentration outside the particle boundary layer, i.e. normally at about 1 mm away from the surface as given by $y^+ = 30$. If the concentration is calculated using CFD, C_∞ might be thought of as the concentration in the cell next to the surface. If the concentration is known only at a much higher height than $y^+ = 30$, i.e. coarser grid, v_d should be modified with the aerodynamic resistance up to that level or, alternatively, the concentration could be extrapolated down to $y^+ = 30$. Regarding the calculation of concentration in an urban area, it could also be noted that Belcher in his review [55] highlighted the role of mean transport within the urban network and concluded that mixing by turbulence was shown to be weaker than, for example, topological dispersion. This opinion was also supported by Zhang, Arya and Snyder [54], who concluded that mean advection plays a more important role than turbulent diffusion, in particular in strongly stratified flows. These conclusions favor flows that might produce hotspots in the deposition pattern and thus emphasis the importance of a good understanding of how the local deposition velocity varies for various conditions, in particular with regard to dispersion of hazardous materials.

5. Conclusions

Micro-scale deposition models from the literature, typically used for pipes, were adapted to outdoor situations and combined with computational fluid dynamics (CFD) calculations of flow conditions in order to study the fine structure of the deposition velocity on ground, roofs and walls. Four geometric cases were simulated: (i) "square houses 90 degrees", (ii) "square houses 45 degrees", (iii) "long houses 90 degrees" and (iv) "long houses 45 degrees". The calculations show large variations of v_d similar to the variation of the friction velocity u_τ demonstrating the strong dependence of v_d on u_τ. Further variation is caused by the variation of the micro-scale roughness and different surface temperatures. For 5 μm particles (density 1300 kg m^{-3}) the range of v_d was 1–4 mm s^{-1} on ground and roofs with hotspots up to 10–60 mm s^{-1}. The main variation of v_d on walls is 0.5–8 mm s^{-1} with hotspots up several cm s^{-1} occurring near the edges and close to the wall/ground boundary. Compared to available observations and other models these values seem reasonable. However, no experimental investigation seems to have studied the fine structure and hotspots of v_d.

The presented results gives some guidance where to look for hotspots of deposited material and also shows that a representation of v_d in a city by only one or just a few values is a great simplification on the local level and could lead to significant errors.

Acknowledgements

The authors gratefully acknowledge the support of Dr Agneta H. Palmboeck, Project manager 'Radiological threat assessments' at FOI, for her helpful comments and suggestions.

References

[1] F. Monforti, R. Bellasio, R. Bianconi, G. Clai, G. Zanini, An evaluation of particle deposition fluxes to cultural heritage sites in Florence, Italy, Sci. Total Environ. 334–335 (2004) 61–72.
[2] J.G. Slowik, K. Steinken, P. Davidovits, L.R. Williams, J.T. Jayne, D.E. Kolb, D.R. Worsnop, Y. Rudich, P.F. DeCarlo, Particle moephology and density characterization by combined mobility and aerodynamic diameter. measurements. Part2. Application to combustions-generated soot aerosols as a function of fuel equivalence ratio, Aerosol Sci. Technol. 38 (2004) 1206–2122.
[3] L. Nordlander, A. Norqvist, R. Roffey, G. Sandström, A. Sjöstedt (Eds.), FOA Briefing Book on Biological Weapons, FOA, Stockholm, 1995.
[4] L.S. Tisa, T. Koshikawa, P. Gerhardt, Wet and dry bacterial spore densities determined by buoyant sedimentation, Appl. Environ. Microbiol. 43 (1982) 1307–1310.
[5] M.R. Sippola, W.W. Nazaroff, Particle deposition from turbulent flow: review of published research and its applicability to ventilation ducts in commercial buildings, Lawrence Berkeley National Laboratory, Report LBNL-51432, 2002.
[6] W.G.N. Slinn, Prediction for particle deposition to vegetative canopies, Atmos. Environ. 16 (1982) 1785–1794.
[7] L. Zhang, S. Gong, J. Padro, L. Barrie, A size-segregated particle dry deposition scheme for an atmospheric aerosol module, Atmos. Environ. 35 (2001) 549–560.
[8] A.C. Wells, A.C. Chamberlain, Transport of small particles to vertical surfaces, Br. J. Appl. Phys. 18 (1967) 1793.
[9] A.C. Chamberlain, J.A. Garland, A.C. Wells, Transport of gases and particles to surfaces with widely spaced roughness elements, Boundary-Layer Meteorol. 29 (1984) 343–360.
[10] B.Y.H. Liu, J.K. Agarwal, Experimental observation of aerosol deposition in turbulent flow, J. Aerosol Sci. 5 (1974) 145–155.
[11] M.R. Sippola, W.W. Nazaroff, Modeling particle loss in ventilation ducts, Atmos. Environ. 37 (2003) 5597–5609.
[12] S.K. Friedlander, H.F. Johnstone, Deposition of suspended particles from turbulent gas streams, Ind. Eng. Chem. 49 (1957) 1151.
[13] C.N. Davies (Ed.), Aerosol Science, Academic Press, London, 1966.
[14] N.B. Wood, A simple method for the calculation of turbulent deposition to smooth and rough surfaces, J. Aerosol Sci. 12 (1981) 275–290.
[15] F.-G. Fan, G. Ahmadi, A sublayer model for turbulent deposition of particles in vertical ducts with smooth and rough surfaces, J. Aerosol Sci. 24 (1993) 45–64.
[16] F.-G. Fan, G. Ahmadi, On the sublayer model for turbulent deposition of aerosol particles in the presence of gravity and electric fields, Aerosol Sci. Technol. 21 (1994) 49–71.
[17] A. Guha, A unified Eulerian theory of turbulent deposition to smooth and rough surfaces, J. Aerosol Sci. 28 (8) (1997) 1517–1537.
[18] J.R. Valentine, P.J. Smith, Numerical Predictions of Deposition with a Particle Cloud Tracking Technique, Reaction Engineering International, Salt Lake City, 2005, http://www.reaction-eng.com/downloads/deposit.pdf.
[19] B. Zhao, J. Wu, Modelling particle deposition from fully developed turbulent flow in ventilation duct, Atmos. Environ. 40 (2006) 457–466.
[20] S.T. Johansen, The deposition of particles on vertical walls, Int. J. Multiphase Flow 17 (1991) 355–376.
[21] Z.Y. Offer, D. Goossens, Wind tunnel experiments and field measurements of aeolian dust deposition on conical hills, Geomorphology 14 (1995) 43–56.
[22] E. Erell, H. Tsoar, Spatial variations in the aeolian deposition of dust—the effect of a city: a case study in Be'er-Sheva, Israel, Atmos. Environ. 33 (1999) 4049–4055.
[23] S.A. Simmons, R.L. Pocock, Spatial variation in heavy metal deposition rates in urban areas, Sci. Total Environ. 59 (1987) 243–251.
[24] M. Benett, A simple physical model of dry deposition to a rough surface, Atmos. Environ. 22 (1988) 2701–2705.
[25] L. Gidhagen, C. Johansson, J. Langner, G. Olivares, Simulation of NO_x and ultrafine particles in a street canyon in Stockholm, Sweden, Atmos. Environ. 38 (2004) 2029–2044.
[26] A.C. Chamberlain, Transport of Lycopodium spores and other small particles to rough surfaces, Proc. R. Soc. Lond. A296 (1966) 45–70.
[27] N.B. Wood, The mass transfer of particles and acid vapour to cooled surfaces, J. Inst. Energy 76 (1981) 76–93.
[28] W. Kvasnak, G. Ahmadi, Deposition of ellipsoidal particles in turbulent duct flows, Chem. Eng. Sci. 51 (1996) 5137–5148.
[29] M. Caporaloni, F. Tampieri, F. Trombetti, O. Vittori, Transfer of particles in nonisotropic air turbulence, J. Aerosol Sci. 32 (1975) 565–568.
[30] J.O. Hinze, Turbulence, second ed., McGraw-Hill, New York, 1975.
[31] E. Kreyszig, Advanced Engineering Mathematics, eighth ed., Wiley, New York, 1999.
[32] C.K. Lai, W.W. Nazaroff, Modeling indoor particle deposition from turbulent flow onto smooth surfaces, J. Aerosol Sci. 31 (2000) 463–476.
[33] G.A. Kallio, M.W. Reeks, A numerical simulation of particle deposition in turbulent boundary layers, Int. J. Multiphase Flow 15 (1989) 433–446.
[34] K.H. Im, P.M. Chung, Particulate deposition from turbulent parallel streams, AIChE J. 29 (1983) 498.
[35] C.M. Tchen, Mean value correlation problems connected with the motion of small particles suspended in a turbulent fluid, Ph.D. Thesis, Delft, 1947.
[36] J.C. Klewicki, On the interactions between the inner and outer region motions in turbulent boundary layers, Ph.D. Thesis, Department of Mechanical Engineering, Michigan State University, 1989.
[37] M. Shimada, K. Okuyama, M. Asai, Deposition of submicron aerosol particles in turbulent and transitional flow, AIChE J. 39 (1993) 17.
[38] J.W. Cleaver, B. Yates, A sub-layer model for the deposition of particles from a turbulent flow, Chem. Eng. Sci. 30 (1975) 983–992.
[39] S.K. Friedlander, Smoke, Dust and Haze: Fundamentals of Aerosol Behavior, John Wiley & Sons, New York, 1977.
[40] J.T. Davies, A new theory of aerosol deposition from turbulent fluids, Chem. Eng. Sci. 38 (1983) 135–139.
[41] P.G. Papavergos, A.B. Hedley, Particle deposition behavior from turbulent flows, Chem. Eng. Des. 62 (1984) 275–295.
[42] T. Kneen, W. Strauss, Deposition of dust from turbulent gas streams, Atmos. Environ. 3 (1969) 55–67.
[43] S.V. Patankar, Numerical Heat Transfer and Fluid Flow, Hemispere Publishing Corp., New York, 1980.
[44] B.E. Launder, D.B. Spalding, Mathematical Models of Turbulence, Academic Press, London, 1972.
[45] Y.S. Chen, S.W. Kim, Computation of turbulent flows using an extended k–ε turbulence closure model, NASA CR-179204, 1987.
[46] D.J. Monson, H.L. Seegmiller, P.K. McConnaughey, Y.S. Chen, Comparison of experiment with calculations using curvature-corrected zero and two-equation turbulence models for a two-dimensional U-duct, AIAA 90-1484, 1990.
[47] R. Hosker, Flow and diffusion near obstacles, Atmospheric Science and Power Production, USDOE, 1984.
[48] M.J. Brown, G.E. Streit, Emergency Responders' "Rules-of-Thumb" for Air Toxic Releases in Urban Environments, LA-UR-98-4539, 1998.
[49] R. Röckle, Bestimmung der Strömungsverhältnisse im Bereich komplexer Bebauungsstrukturen, Dissertation, Vom Fachbereich Mechanik, der Technischen Hochschule Darmstadt, 1990.
[50] C.-H. Chang, R.N. Meroney, Numerical and physical modelling of bluff body flow and dispersion in urban street canyons, J. Wind Energy Ind. Aerodyn. 89 (2001) 1325–1334.
[51] M. Pavageau, M. Schatzmann, Wind tunnel measurements of concentration fluctuations in an urban street canyon, Atmos. Environ. 33 (1999) 3961–3971.

[52] G.T. Johnson, L.J. Hunter, Some insights into typical urban canyon airflows, Atmos. Environ. 33 (1999) 3991–3999.
[53] W.H. Snyder, Some observations of the influence of stratification on diffusion in building wakes, in: I.P. Castro, N.J. Rockliff (Eds.), Stably stratified Flows: Flow and Dispersion over Topography, Clarendron Press, Oxford, 1994, pp. 301–324.
[54] Y.Q. Zhang, S.P. Arya, W.H. Snyder, A comparison of numerical and physical modelling of stable atmospheric flow and dispersion around a cubical building, Atmos. Environ. 30 (1996) 1327–1345.
[55] S.E. Belcher, Mixing and transport in urban areas, Philos. Trans. R. Soc. A 363 (2005) 2947–2968.